PHYSICAL REVIEW D **95,** 074020 (2017)

Photoproduction of doubly heavy baryon at the LHeC

Huan-Yu Bi,[1,†] Ren-You Zhang,[1,*] Xing-Gang Wu,[2,‡] Wen-Gan Ma,[1,§] Xiao-Zhou Li,[1,‖] and Samuel Owusu[1,¶]

[1]*Department of Modern Physics, University of Science and Technology of China, Hefei, Anhui 230026, People's Republic of China*

[2]*Department of Physics, Chongqing University, Chongqing 401331, People's Republic of China*

(Received 7 March 2017; published 14 April 2017)

The photoproduction of doubly heavy baryon, Ξ_{cc}, Ξ_{bc}, and Ξ_{bb}, is predicted within the nonrelativistic QCD at the Large Hadron Electron Collider (LHeC). The $\Xi_{QQ'}$ production via the photon-gluon fusing channel $\gamma + g \to \langle QQ' \rangle[n] + \bar{Q} + \bar{Q}'$ and the extrinsic heavy quark channel $\gamma + Q \to \langle QQ' \rangle[n] + \bar{Q}'$ have been considered, where Q or Q' stand for heavy c or b quark and $\langle QQ' \rangle[n]$ stands for a QQ' diquark with given spin- and color- configurations $[n]$. The diquark shall fragmentate into $\Xi_{QQ'}$ baryon with high probability. For Ξ_{cc} and Ξ_{bb} production, $[n]$ equals $[^1S_0]_{\mathbf{6}}$ (in configurations spin-singlet $^1S_0$-wave and color-sextuplet $\mathbf{6}$) or $[^3S_1]_{\bar{\mathbf{3}}}$ (in configurations spin-triplet $^3S_1$-wave and color-antitriplet $\bar{\mathbf{3}}$) and for Ξ_{bc} production, $[n]$ equals $[^1S_0]_{\bar{\mathbf{3}}}$, $[^1S_0]_{\mathbf{6}}$, $[^3S_1]_{\bar{\mathbf{3}}}$, or $[^3S_1]_{\mathbf{6}}$. A detailed comparison of those channels and configurations on total and differential cross sections, together with their uncertainties, is presented. We find the dominant contributions for $\Xi_{QQ'}$ production are from extrinsic heavy quark channel and for $[^3S_1]_{\bar{\mathbf{3}}}$ configuration, while other diquark states can also provide sizable contributions to the $\Xi_{QQ'}$ production. As a combination of all the mentioned channels and configurations and by taking $m_c = 1.80 \pm 0.10$ GeV and $m_b = 5.1 \pm 0.20$ GeV, we observe that $(6.70^{+1.40}_{-1.10}) \times 10^3$ Ξ_{bb}, $(8.81^{+3.08}_{-2.20}) \times 10^6$ Ξ_{cc}, and $(4.63^{+1.21}_{-0.92}) \times 10^5$ Ξ_{bc} events can be generated at the LHeC in one operation year with colliding energy $\sqrt{S} = 1.30$ TeV and luminosity $\mathcal{L} \simeq 10^{33}$ cm^{-2} s^{-1}. Thus, the LHeC shall help us to get more information about the doubly heavy baryon, especially for Ξ_{cc} and Ξ_{bc}.

DOI: 10.1103/PhysRevD.95.074020

I. INTRODUCTION

The heavy-quark mass provides a natural hard scale, so the processes involving heavy quarks are perturbative QCD (pQCD) calculable by applying proper factorization theories. Among them, the nonrelativistic quantum chromodynamics (NRQCD) [1] provides a powerful approach to study the properties of doubly heavy hadrons, since their heavy constituent quarks move nonrelativistically in the bound system [2,3]. Recently, we have studied the photoproduction of B_c meson at the Large Hadron Electron Collider (LHeC) [4] within the framework of NRQCD, and it was found that sizable amounts of B_c meson events can be generated [5]. As a step forward, we shall investigate whether sizable amounts of doubly heavy baryon events can also be produced at the LHeC. If so, to compare with future possible data, it could be inversely treated as a platform for testing the effectiveness of NRQCD.

For doubly heavy baryons Ξ_{cc}, Ξ_{bc}, and Ξ_{bb}, only Ξ_{cc} was observed in the fixed target experiment by the SELEX collaboration [6–8], which however has not been confirmed by other experiments so far. Here and henceforth, for simplicity, we use $\Xi_{QQ'}$ to denote the doubly heavy baryon $\Xi_{QQ'q}$, where q stands for a light quark u, d, or s, respectively. At present, most of the predictions on the production rate and decay width are well underestimated compared to the SELEX measurements [9–18]. The unexpected high production rate of Ξ_{cc} baryons may be due to the kinematics features of the SELEX experiment, and could not be described by the production mechanism only [19]. Thus, to understand the properties of doubly heavy baryon better, experimentally, we need to accumulate more events to reduce the statistical error; and theoretically, it is important to make a systematic research on various production mechanism of doubly heavy baryon at different experimental platforms.

A dedicated generator GENXICC [20–22] was developed and has been applied to study the production of doubly heavy baryon at the hadronic colliders [23,24]. In 2013, the LHCb collaboration at the LHC performed their first search of Ξ_{cc}, but no significant signal has been found [25]. Future searches at the LHC with improved trigger conditions and larger data samples should improve the sensitivity significantly. In addition, series predictions on the production of doubly heavy baryon at the high luminosity electron-electron colliders, such as the Z-factory [26] and the International Linear Collider (ILC) [27], have also been

*Corresponding author.
zhangry@ustc.edu.cn
†bihy@mail.ustc.edu.cn
‡wuxg@cqu.edu.cn
§mawg@ustc.edu.cn
‖lixiaozhou@ustc.edu.cn
¶samuel@mail.ustc.edu.cn

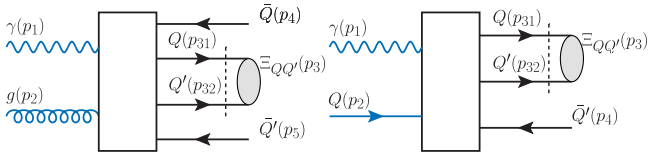

FIG. 1. Schematic diagrams for the photoproduction of $\Xi_{QQ'}$ at the LHeC. The box stands for the hard interaction kernel of $Q\bar{Q}$ ($Q'\bar{Q}'$)-pair production.

performed. Sizable amounts of doubly heavy baryon events are expected to be generated in those platforms [28–31].

In addition, the hadron-lepton collider may also be a possible machine to probe the properties of the doubly heavy baryons. As clarified in Refs. [4,5], the photoproduction mechanism dominates the production of c/b-quark at the LHeC, and the doubly heavy baryon can thus be mainly generated via the photoproduction channels $\gamma + g \to \Xi_{QQ'} + \bar{Q} + \bar{Q}'$ and $\gamma + Q \to \Xi_{QQ'} + \bar{Q}'$.

Schematic diagrams for the photoproduction of $\Xi_{QQ'}$ at the LHeC are shown in Fig. 1. The photoproduction of $\Xi_{QQ'}$ can be divided into three steps. Taking $\gamma + g$ channel as an example, the first step is the production of $Q\bar{Q}$ and $Q'\bar{Q}'$ pairs, where the heavy quarks Q and Q' are required to be in the color- and spin-configuration $[n]$; The second step is the $(QQ')[n]$ pair fuses into a binding diquark $\langle QQ'\rangle[n]$ with certain probability; The third step is the evolution of the diquark into a doubly heavy baryon $\Xi_{QQ'}$ by grabbing a light quark from the "vacuo" or emitting/grabbing a suitable number of gluons. The first step is perturbatively calculable since the gluon should be hard enough to generate the heavy quark-antiquark pair. For the second step, the transition probability can be described by a nonperturbative NRQCD matrix element. We use $h_{\mathbf{6}}$ and $h_{\bar{\mathbf{3}}}$ to stand for the matrix elements of the production of a color-sextuplet ($\mathbf{6}$) and a color-antitriplet ($\bar{\mathbf{3}}$) diquark, respectively.[1] For the third step, one usually assumes the efficiency of evolution from a $\langle QQ'\rangle[n]$ diquark to a doubly heavy baryon $\Xi_{QQ'}$ is 100%, referring as the "direct evolution." Reference [31] has studied the evolution through direct evolution as well as "evolution via fragmentation" in which the fragmentation function has been taken into account. The authors there have found that the direct evolution is of high precision and is sufficient enough for studying the production of doubly heavy baryon, and thus we adopt the direct evolution in our calculation.

Since the predicted production rate of Ξ_{cc} are much smaller than the SELEX measurements, the authors of Refs. [15,16,20] suggested to take into account the extrinsic and intrinsic charm production mechanism such that to shrink the gaps between theoretical and experimental predictions. It is noted that the intrinsic charm's contribution to the cross section of $\gamma + c$ channel is less than 0.1% even if the density of intrinsic c-component in proton is up to 1% [32,33]. According to our experience on the B_c meson photoproduction and following the suggestion given in Refs. [15,20], we shall concentrate our attention on the channels $\gamma + g \to \Xi_{QQ'} + \bar{Q} + \bar{Q}'$ and $\gamma + Q \to \Xi_{QQ'} + \bar{Q}'$, in which the intermediate diquark $\langle QQ'\rangle[n]$ is $\langle cc/bb\rangle[^1S_0]_{\mathbf{6}}$, $\langle cc/bb\rangle[^3S_1]_{\bar{\mathbf{3}}}$, $\langle bc\rangle[^1S_0]_{\bar{\mathbf{3}}/\mathbf{6}}$, and $\langle bc\rangle[^3S_1]_{\bar{\mathbf{3}}/\mathbf{6}}$, respectively. Other diquark configurations $\langle cc/bb\rangle[^3S_1]_{\mathbf{6}}$ and $\langle cc/bb\rangle[^1S_0]_{\bar{\mathbf{3}}}$ are forbidden due to the Fermi-Dirac statistics for identical particles.

The rest of the paper is organized as follows. In Sec. II, we present the formulations for dealing with the subprocesses $\gamma + g \to \Xi_{QQ'} + \bar{Q} + \bar{Q}'$ and $\gamma + Q \to \Xi_{QQ'} + \bar{Q}'$ in detail. Numerical results, theoretical uncertainties and discussions are given in Sec. III. Finally, a brief summary is given in Sec. IV.

II. CALCULATION TECHNOLOGY

A. Basic formulas

For the photoproduction mechanism, the initial photon is emitted from the electron, which can be described by the Weizsäcker-Williams approximation (WWA) [34–36]. When considering the extrinsic heavy-quark mechanism, we should pay special attention to avoid the "double counting" problem between the $\gamma + g$ and the extrinsic $\gamma + Q$ channels. A proper approach to deal with the extrinsic heavy quark is to employ the general-mass variable-flavor-number scheme (GM-VFNs) [37–41]. According to the pQCD factorization theorem, the cross section for the photoproduction of $\Xi_{QQ'}$ within the GM-VFNs scheme can be written as

$$
\begin{aligned}
&d\sigma(e^- + P \to \Xi_{QQ'} + X) \\
&= \sum_{[n]} \langle \mathcal{O}^{\langle QQ'\rangle}[n]\rangle \Big\{ f_{\gamma/e^-}(x_1) f_{g/P}(x_2,\mu_f) \otimes d\hat{\sigma}(\gamma + g \to (QQ')[n] + X) \\
&\quad + f_{\gamma/e^-}(x_1)[(f_{Q/P}(x_2,\mu_f) - f_{Q/P}(x_2,\mu_f)_{\mathrm{SUB}}) \otimes d\hat{\sigma}(\gamma + Q \to (QQ')[n] + X) + Q \leftrightarrow Q'] \frac{1}{1+\delta_{QQ'}} \Big\}, \qquad (1)
\end{aligned}
$$

[1]Here, we don't distinguish the matrix elements of $^1S_0$ and $^3S_1$ states, since the spin-splitting effect is small [23,28].

where $f_{\gamma/e^-}(x_1)$ is the WWA photon density function, $f_{i/P}(x_2,\mu_f)$ is the parton distribution function (PDF) of parton i inside a proton P, μ_f is the factorization scale, and $d\hat{\sigma}(\gamma+i\to(QQ')[n]+X)$ is the hard cross section for the partonic process $\gamma+i\to(QQ')[n]+X$. $\langle\mathcal{O}^{\langle QQ'\rangle}[n]\rangle$ is the nonperturbative matrix element which represents the transition probability from the $(QQ')[n]$-quark pair to the desired baryon $\Xi_{QQ'}$. $\delta_{QQ'}=1(0)$ for $Q=Q'$ $(Q\neq Q')$. Since we adopt the direct evolution scheme, we have $\langle\mathcal{O}^{\langle QQ'\rangle}[n]\rangle=h_{\bar{\mathbf{3}}}$ or $h_{\mathbf{6}}$, respectively.

The photon density function depicted by the WWA is expressed as [34–36]

$$f_{\gamma/e^-}(x)=\frac{\alpha}{2\pi}\left[\frac{1+(1-x)^2}{x}\ln\frac{Q^2_{\max}}{Q^2_{\min}}+2m_e^2x\left(\frac{1}{Q^2_{\max}}-\frac{1}{Q^2_{\min}}\right)\right],\tag{2}$$

where $x=E_\gamma/E_e$, E_γ, and E_e are photon and electron energies. α is the fine structure constant and m_e is the electron mass. $Q^2_{\min}$ and $Q^2_{\max}$ are given by

$$Q^2_{\min}=\frac{m_e^2x^2}{1-x},\qquad Q^2_{\max}=(\theta_cE_e)^2(1-x)+Q^2_{\min},\tag{3}$$

where the electron scattering angle cut θ_c is determined by experiment [42,43].

The subtraction term $f_{Q/P}(x_2,\mu_f)_{\rm SUB}$ in Eq. (1) is defined as

$$f_{Q/p}(x_2,\mu_f)_{\rm SUB}=\int_{x_2}^1 f_{g/P}(x_2/y,\mu_f)f_{Q/g}(y,\mu_f)\frac{dy}{y},\tag{4}$$

where $f_{Q/g}(y,\mu_f)$ is the Q-quark distribution function within an on-shell gluon and it can be expanded order by order in α_s. At the α_s-order, $f_{Q/g}(y,\mu_f)$ is given by

$$f_{Q/g}(y,\mu_f)=\frac{\alpha_s(\mu_f)}{2\pi}\ln\frac{\mu_f^2}{m_Q^2}P_{g\to Q}(y),\tag{5}$$

where $P_{g\to Q}(y)=\frac{1}{2}(1-2y+2y^2)$ is the $g\to Q\bar{Q}$ splitting function.

The partonic hard cross section can be written as

$$d\hat{\sigma}(\gamma+i\to(QQ')[n]+X)=\frac{\overline{\sum}|\mathcal{M}|^2}{4\sqrt{(p_1+p_2)^2}|\vec{p}_1|}d\Phi_j,\tag{6}$$

where $\overline{\sum}$ denotes the average of the spin and color states of initial particles and the sum of the color and spin states of all final particles, and $d\Phi_j$ represents the final j-body phase space element,

$$d\Phi_j=(2\pi)^4\delta^4\left(p_1+p_2-\sum_{f=3}^{j+2}p_f\right)\prod_{f=3}^{j+2}\frac{d^3p_f}{(2\pi)^3 2p_f^0}\tag{7}$$

and $\mathcal{M}$ is the total hard scattering amplitude

$$\mathcal{M}=\sum_k\mathcal{M}_k,\tag{8}$$

where k runs over the related Feynman diagrams.

B. Feynman diagram and amplitude

There are totally 24 Feynman diagrams for the subprocess $\gamma+g\to(QQ')[n]+\bar{Q}+\bar{Q}'$ $(k=24)$ and 4 Feynman diagrams for the subprocess $\gamma+Q\to(QQ')[n]+\bar{Q}$ $(k=4)$. As for the subprocesses $\gamma+g\to(QQ)[n]+\bar{Q}+\bar{Q}$ and $\gamma+Q\to(QQ)[n]+\bar{Q}$, there are another 24 and 4 diagrams coming from the exchanging of two identical quark lines inside the $(QQ)[n]$-quark pair. Practically, those diagrams are the same as the diagrams without exchanging, since we have set the relative velocity between the two Q quarks to be zero, i.e., we have set $p_{31}=p_{32}=\frac{p_3}{2}$ for the production of Ξ_{QQ} by applying the nonrelativistic approximation. There is a factor of $1/2!$ for the square of the amplitude due to the two identical quarks inside the $\langle QQ\rangle[n]$ diquark. Thus, we only need to calculate the 24 and 4 diagrams for $\gamma+g\to(QQ)[n]+\bar{Q}+\bar{Q}$ and $\gamma+Q\to(QQ)[n]+\bar{Q}$ subprocesses, and multiply a factor of $2^2/2!$ at the cross section level. Besides, there is another factor of $1/2$ for the $\gamma+g\to(QQ)[n]+\bar{Q}+\bar{Q}$ subprocess coming from the two identical open antiquarks $\bar{Q}$ in the final 3-body phase space. The amplitudes for $\gamma+g\to(QQ')[n]+\bar{Q}+\bar{Q}'$ and $\gamma+Q\to(QQ')[n]+\bar{Q}'$ can be obtained directly from the Feynman diagrams. In order to describe the bound system of the doubly heavy baryon, we should apply the spin- and color-projection operators on the amplitude of $(QQ')[n]$-quark pair. For a detailed description on how to apply the projection operators on the amplitude of $(QQ')[n]$-quark pair and the calculation of the color factor of the production of heavy baryon, one can refer to Refs. [5,15].

To implement the calculation, the FeynArts package [44] is used to generate the Feynman diagrams and amplitudes; The FeynCalc [45,46] and FeynCalcFormLink packages [47] are used to handle the Dirac trace and $SU(N_c)$ algebraic calculations. Numerical integrations over 2- and 3-body phase spaces are performed by using the VEGAS [48] and FormCalc [49] packages.

III. NUMERICAL RESULTS AND DISCUSSIONS

A. Input parameters

The matrix element $h_{\bar{\mathbf{3}}}$ is related to the Schrödinger wave function at the origin, $h_{\bar{\mathbf{3}}}=|\Psi_{(QQ')}(0)|^2$ [50]. According to the velocity scaling rule of NRQCD [18], the color-sextuplet matrix element $h_{\mathbf{6}}$ is at the same order of $h_{\bar{\mathbf{3}}}$,

TABLE I. Total cross sections (in unit pb) for the photoproduction of $\Xi_{QQ'}$ at the LHeC and FCC-ep colliders.

⋯	$\sqrt{S}=1.30$ TeV				$\sqrt{S}=1.98$ TeV				$\sqrt{S}=7.07$ TeV				$\sqrt{S}=10.00$ TeV			
⋯	$\langle bb\rangle_{\mathbf{c}}$	$\langle cc\rangle_{\mathbf{c}}$	$\langle bc\rangle_{\bar{\mathbf{3}}}$	$\langle bc\rangle_{\mathbf{6}}$	$\langle bb\rangle_{\mathbf{c}}$	$\langle cc\rangle_{\mathbf{c}}$	$\langle bc\rangle_{\bar{\mathbf{3}}}$	$\langle bc\rangle_{\mathbf{6}}$	$\langle bb\rangle_{\mathbf{c}}$	$\langle cc\rangle_{\mathbf{c}}$	$\langle bc\rangle_{\bar{\mathbf{3}}}$	$\langle bc\rangle_{\mathbf{6}}$	$\langle bb\rangle_{\mathbf{c}}$	$\langle cc\rangle_{\mathbf{c}}$	$\langle bc\rangle_{\bar{\mathbf{3}}}$	$\langle bc\rangle_{\mathbf{6}}$
$\sigma_{\gamma g}$	0.02	21.61	1.55	1.06	0.04	32.81	2.58	1.76	0.16	82.81	7.99	5.39	0.22	108.43	10.95	7.37
$\sigma_{\gamma c}$	⋯	42.91	0.27	0.13	⋯	62.28	0.41	0.20	⋯	140.60	1.00	0.50	⋯	178.84	1.29	0.65
$\sigma_{\gamma b}$	0.02	⋯	3.84	1.92	0.04	⋯	6.38	3.19	0.15	⋯	20.01	10.01	0.21	⋯	27.59	13.80
$\sigma^*_{\gamma g}$	0.29	241.67	5.09	4.32	0.50	360.75	8.43	7.12	1.75	877.57	25.73	21.53	2.46	1139.59	35.17	29.36
$\sigma^*_{\gamma c}$	⋯	574.42	1.26	0.63	⋯	829.44	1.91	0.95	⋯	1854.55	4.62	2.31	⋯	2354.47	5.95	2.97
$\sigma^*_{\gamma b}$	0.34	⋯	17.48	8.74	0.59	⋯	28.98	14.49	2.04	⋯	90.71	45.35	2.86	⋯	125.02	62.51
Total	0.67	880.61	46.29		1.17	1285.28	76.40		4.10	2955.53	235.15		5.75	3781.33	322.63	

and we take the usual choice of $h_{\mathbf{6}}=h_{\bar{\mathbf{3}}}$ to do our calculation. Since $h_{\mathbf{6}/\bar{\mathbf{3}}}$ is an overall factor, one can improve our results once more accurate $h_{\mathbf{6}/\bar{\mathbf{3}}}$ is known. The wave functions at the origin together with the heavy quark masses are taken as follows [11,50]:

$$|\Psi_{(cc)}(0)|^2=0.039\ \mathrm{GeV}^3,\qquad |\Psi_{(bc)}(0)|^2=0.065\ \mathrm{GeV}^3,$$
$$|\Psi_{(bb)}(0)|^2=0.152\ \mathrm{GeV}^3,\qquad m_b=5.1\ \mathrm{GeV},$$
$$m_c=1.8\ \mathrm{GeV}.$$

The electron mass $m_e=0.51\times10^{-3}$ GeV is adopted and the fine-structure constant is fixed as $\alpha=1/137$. The electron scattering angle cut θ_c is chosen as 32 mrad which is consistent with the choices of Refs. [51,52]. The renormalization and factorization scales are set to be the transverse mass of $\Xi_{QQ'}$, $\mu_r=\mu_f=M_T$, where $M_T=\sqrt{p_T^2+M^2}$ with M being the mass of $\Xi_{QQ'}$. Here $M=m_Q+m_{Q'}$, which ensures the gauge invariance of the hard scattering amplitude. The PDF of the incident quark in hadron is taken as CT10NLO [53], and correspondingly, the next-to-leading order α_s-running with $\Lambda^{(4)}_{\mathrm{QCD}}=326$ MeV ($\Lambda^{(5)}_{\mathrm{QCD}}=226$ MeV) is adopted.

B. Basic results

To shorten the notation, we denote the cross sections for the production of $\langle QQ'\rangle[^1S_0]_{\bar{\mathbf{3}}/\mathbf{6}}$ and $\langle QQ'\rangle[^3S_1]_{\bar{\mathbf{3}}/\mathbf{6}}$ via the $\gamma+i$ channels as $\sigma_{\gamma i}$ and $\sigma^*_{\gamma i}$, where $i=g,c,b$ respectively. We use $\langle bc\rangle_{\bar{\mathbf{3}}}$ and $\langle bc\rangle_{\mathbf{6}}$ to represent the production of $\langle bc\rangle[^1S_0/^3S_1]_{\bar{\mathbf{3}}}$ and $\langle bc\rangle[^1S_0/^3S_1]_{\mathbf{6}}$. We use $\langle QQ\rangle_{\mathbf{c}}$ to represent the production of $\langle QQ\rangle[^3S_1]_{\bar{\mathbf{3}}}$ or $\langle QQ\rangle[^1S_0]_{\mathbf{6}}$, since $\langle QQ\rangle[^3S_1]_{\mathbf{6}}$ and $\langle QQ\rangle[^1S_0]_{\bar{\mathbf{3}}}$ are forbidden.

We present the cross sections for the photoproduction of $\Xi_{QQ'}$ at the electron-hadron colliders under various production channels in Table I. Here, to show how the cross section depends on the electron-hadron colliding energy, we present the numerical results at two ep colliders with four colliding energies, i.e., $\sqrt{S}=1.30$ TeV or 1.98 TeV for LHeC which corresponds to $E_e=60$ or 140 GeV and $E_P=7$ TeV [4], and $\sqrt{S}=7.07$ TeV or 10.00 TeV for the future circular collider based ep collider (FCC-ep) which corresponds to $E_e=250$ or 500 GeV and $E_P=50$ TeV [54].

Table I shows

(i) For the same production channel, the $[^3S_1]_{\bar{\mathbf{3}}}$ diquark state provides the largest contribution for the production cross section of $\Xi_{QQ'}$. For the Ξ_{cc} and Ξ_{bb} production, the color-sextuplet $[^1S_0]_{\mathbf{6}}$ diquark state gives about 7%–8% contribution to the total cross section of the same production channel. For the Ξ_{bc} production, contributions from other diquark states are also sizable, especially, the cross section of $[^3S_1]_{\mathbf{6}}$ diquark state is close to that of $[^3S_1]_{\bar{\mathbf{3}}}$. Thus a careful discussion of all diquark configurations are helpful for a sound prediction of the doubly heavy baryon production.

(ii) In addition to the usually considered $\gamma+g$ channel, the extrinsic heavy quark mechanism via the $\gamma+Q$ channel shall also provide sizable contribution to the production cross section. For example, the $\gamma+c$ channel is even dominant over the $\gamma+g$ channel for the Ξ_{cc} production. This dominance, as shall be

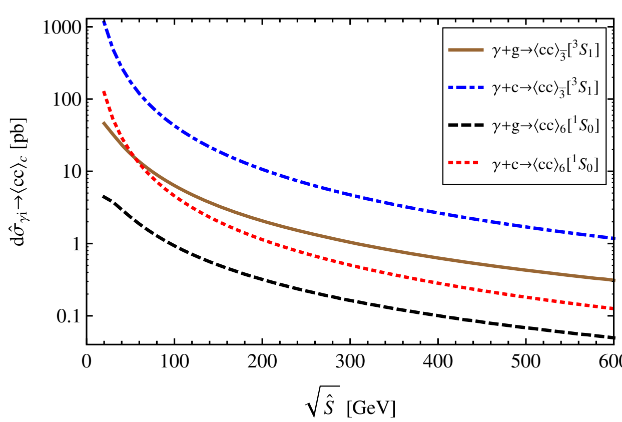

FIG. 2. Partonic cross sections for the photoproduction of $\Xi_{QQ'}$ versus $\sqrt{\hat{s}}$.

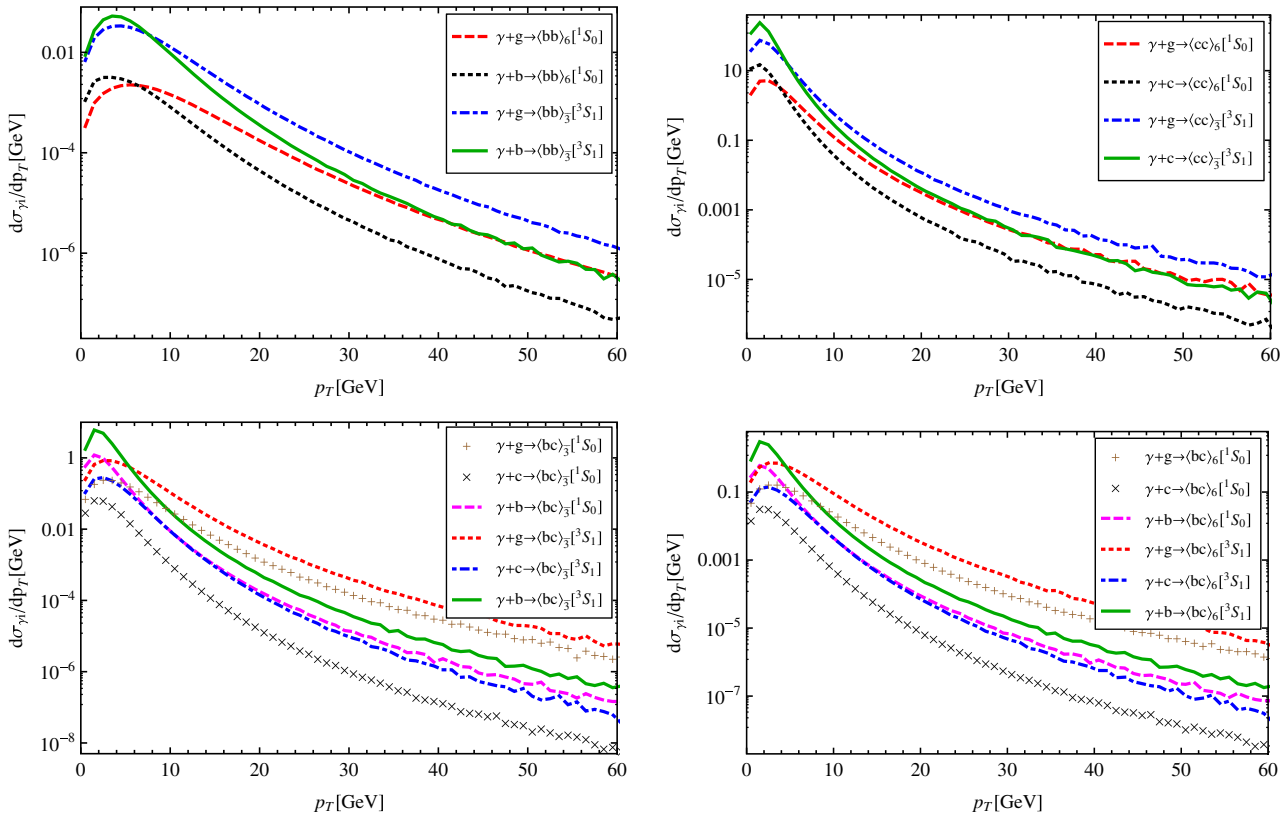

FIG. 3. Transverse momentum distributions for the photoproduction of $\Xi_{QQ'}$ at the $\sqrt{S} = 1.30$ TeV LHeC.

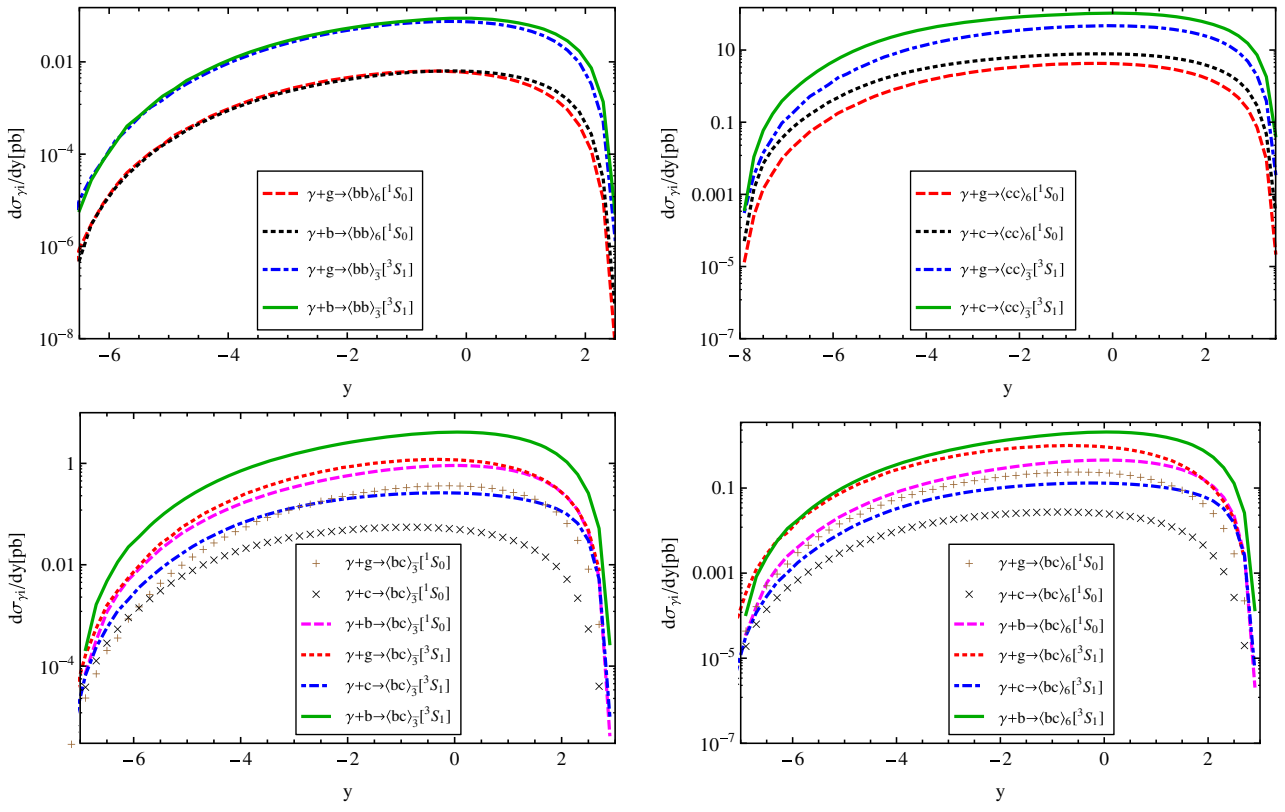

FIG. 4. Rapidity distributions for the photoproduction of $\Xi_{QQ'}$ at the $\sqrt{S} = 1.30$ TeV LHeC.

TABLE II. Total cross sections (in unit pb) for the photoproduction of $\Xi_{QQ'}$ at the $\sqrt{S} = 1.30$ TeV LHeC under various p_T cuts.

⋯	$p_T \geq 1$ GeV				$p_T \geq 3$ GeV				$p_T \geq 5$ GeV			
⋯	$\langle bb\rangle_{\mathbf{c}}$	$\langle cc\rangle_{\mathbf{c}}$	$\langle bc\rangle_{\bar{\mathbf{3}}}$	$\langle bc\rangle_{\mathbf{6}}$	$\langle bb\rangle_{\mathbf{c}}$	$\langle cc\rangle_{\mathbf{c}}$	$\langle bc\rangle_{\bar{\mathbf{3}}}$	$\langle bc\rangle_{\mathbf{6}}$	$\langle bb\rangle_{\mathbf{c}}$	$\langle cc\rangle_{\mathbf{c}}$	$\langle bc\rangle_{\bar{\mathbf{3}}}$	$\langle bc\rangle_{\mathbf{6}}$
$\sigma_{\gamma g}$	0.02	19.46	1.47	1.01	0.02	9.34	1.03	0.71	0.02	3.26	0.57	0.39
$\sigma_{\gamma c}$	⋯	31.45	0.24	0.12	⋯	7.48	0.11	0.05	⋯	1.52	0.03	0.02
$\sigma_{\gamma b}$	0.02	⋯	3.27	1.63	0.02	⋯	1.08	0.54	0.01	⋯	0.28	0.14
$\sigma^*_{\gamma g}$	0.28	203.55	5.09	4.11	0.23	70.07	3.35	2.85	0.16	18.81	1.82	1.55
$\sigma^*_{\gamma c}$	⋯	454.38	1.16	0.58	⋯	82.11	0.62	0.31	⋯	13.30	0.24	0.12
$\sigma^*_{\gamma b}$	0.33	⋯	15.73	7.87	0.26	⋯	4.76	2.38	0.15	⋯	1.11	0.56
Total	0.65	708.84	42.28		0.53	169.00	17.79		0.34	36.89	6.83	

shown later, is caused by the dominance of the $\gamma + Q$ channel in low p_T region.

(iii) By summing up all the mentioned diquark configurations and production channels, we obtain $\sigma^{\rm Total}_{\langle cc\rangle} \gg \sigma^{\rm Total}_{\langle bc\rangle} \gg \sigma^{\rm Total}_{\langle bb\rangle}$, which agrees with the observation of the doubly heavy baryon production at the ILC [31].

(iv) The total cross section increases with the increment of electron-proton colliding energy, differing to the doubly heavy baryon production at the ILC [31], where the total cross section decreases with the increment of electron-positron colliding energy. However, the partonic cross sections for the photoproduction of $\Xi_{QQ'}$ at both ILC and LHeC (i.e., $\gamma + \gamma \to \Xi_{QQ'} + X$ and $\gamma + i \to \Xi_{QQ'} + X$) decrease with the increment of the parton-parton colliding energy. For example, we present the dependence of the partonic cross sections for $\gamma + i \to \Xi_{cc} + X$ on the partonic colliding energy in Fig. 2.

We have found that the photoproduction of $\Xi_{QQ'}$ are similar under various electron-proton collision energies. In the following, we take $\sqrt{S} = 1.30$ TeV as an explicit example to show the photoproduction of $\Xi_{QQ'}$ in detail.

We present the transverse momentum (p_T) distributions for the photoproduction of $\Xi_{QQ'}$ in Fig. 3. The p_T distribution for each channel has a peak for $p_T \sim \mathcal{O}(1)$ GeV and then drops down logarithmically. The p_T distributions of the $\gamma + c$ and $\gamma + \bar{b}$ channels descend more quickly than those of $\gamma + g$ channels in high p_T region. For the $\Xi_{QQ'}$ production via the same diquark configuration, the $\gamma + Q$ channel dominates the $\gamma + g$ channel in small p_T region, which explains sizable total cross section of $\gamma + Q$ channel as shown in Table I. We also observe that the p_T distributions of Ξ_{bb} decrease more slowly than those of Ξ_{bc} and Ξ_{cc} with the increment of p_T, and thus the Ξ_{bb} events may be comparable to Ξ_{cc} and Ξ_{bc} at high p_T region, although the total cross section of Ξ_{bb} is much smaller than those of Ξ_{cc} and Ξ_{bc}.

We present the rapidity (y) distributions for the photoproduction of $\Xi_{QQ'}$ in Fig. 4. The asymmetry of the rapidity distributions of $\Xi_{QQ'}$ clearly shows that the dominant contribution appears in the region of $y < 0$. The z-axis is defined in the direction of the electron beam, thus the fact of $y < 0$ implies the parton i from the proton is more energetic than the photon, and most of $\Xi_{QQ'}$ events tend to be produced in the direction of the proton beam.

We present the cross sections under various p_T and y cuts in Tables II and III. Table II shows the cross section of Ξ_{bc} and Ξ_{cc} under various of p_T cuts are more sensitive than that of Ξ_{bb}, which is consistent with Fig. 3. Table II

TABLE III. Total cross sections (in unit pb) for the photoproduction of $\Xi_{QQ'}$ at the $\sqrt{S} = 1.30$ TeV LHeC under various y cuts.

⋯	$\lvert y\rvert \leq 1$				$\lvert y\rvert \leq 2$				$\lvert y\rvert \leq 3$			
⋯	$\langle bb\rangle_{\mathbf{c}}$	$\langle cc\rangle_{\mathbf{c}}$	$\langle bc\rangle_{\bar{\mathbf{3}}}$	$\langle bc\rangle_{\mathbf{6}}$	$\langle bb\rangle_{\mathbf{c}}$	$\langle cc\rangle_{\mathbf{c}}$	$\langle bc\rangle_{\bar{\mathbf{3}}}$	$\langle bc\rangle_{\mathbf{6}}$	$\langle bb\rangle_{\mathbf{c}}$	$\langle cc\rangle_{\mathbf{c}}$	$\langle bc\rangle_{\bar{\mathbf{3}}}$	$\langle bc\rangle_{\mathbf{6}}$
$\sigma_{\gamma g}$	0.01	8.11	0.71	0.45	0.02	14.52	1.21	0.77	0.02	18.30	1.42	0.93
$\sigma_{\gamma c}$	⋯	15.18	0.10	0.05	⋯	27.65	0.18	0.09	⋯	35.46	0.22	0.11
$\sigma_{\gamma b}$	0.01	⋯	1.73	0.86	0.02	⋯	2.94	1.47	0.02	⋯	3.48	1.74
$\sigma^*_{\gamma g}$	0.14	91.18	2.23	1.76	0.23	165.01	3.80	3.01	0.26	208.64	4.56	3.72
$\sigma^*_{\gamma c}$	⋯	203.34	0.50	0.25	⋯	373.08	0.90	0.45	⋯	480.93	1.11	0.56
$\sigma^*_{\gamma b}$	0.16	⋯	7.85	3.93	0.27	⋯	13.42	6.71	0.31	⋯	15.84	7.92
Total	0.32	317.81	20.42		0.54	480.26	34.95		0.61	743.33	41.61	

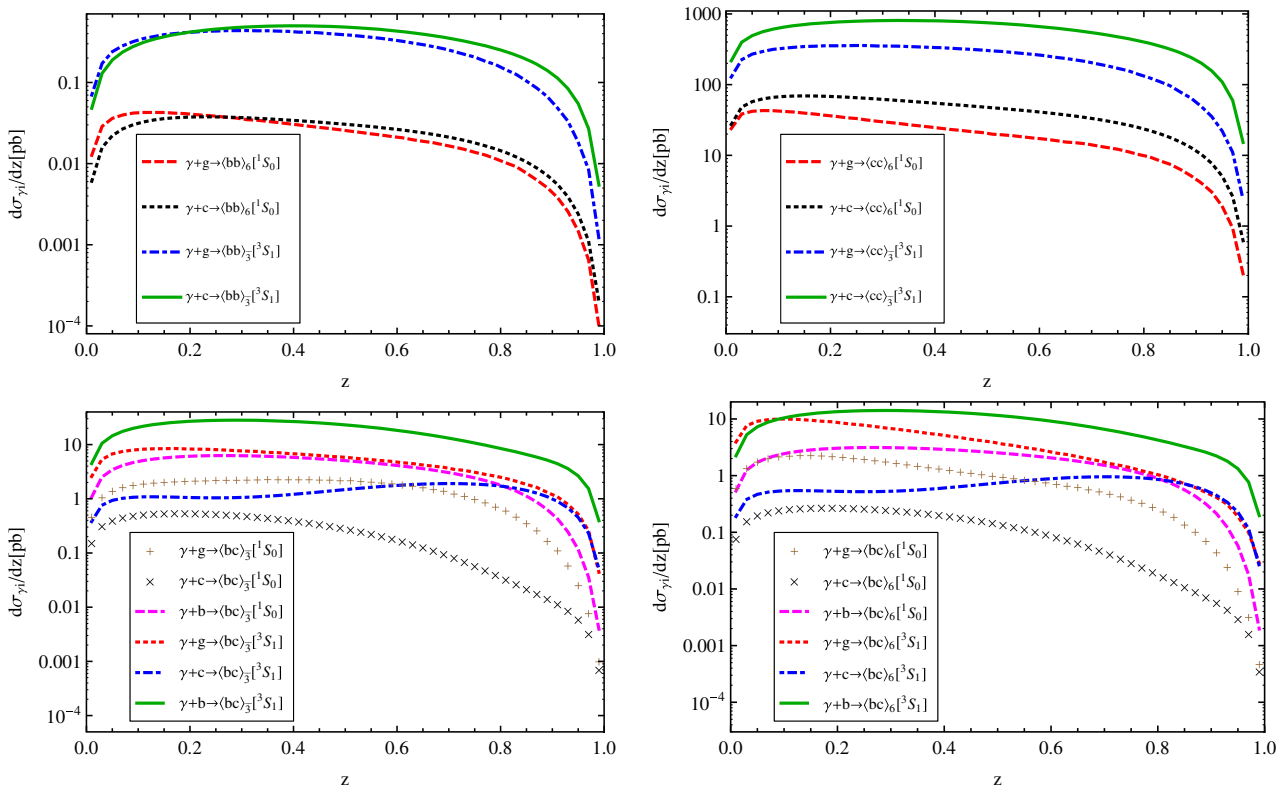

FIG. 5. z distributions for the photoproduction of $\Xi_{QQ'}$ at the $\sqrt{S} = 1.30$ TeV LHeC.

shows notable Ξ_{bc} and Ξ_{cc} production rate can be generated even with a large p_T cut.

Finally, we draw the differential cross sections $d\sigma/dz$ for various diquark configurations and production channels in Fig. 5, where $z = \frac{p_\Xi \cdot p_P}{p_\gamma \cdot p_P}$. Here, p_γ, p_P, and p_Ξ are four momenta of the photon, proton, and $\Xi_{QQ'}$ respectively. For elastic/diffractive events, z is close to 1 [55], besides, at low z region, the resolved effect should be taken into consideration [56]. For the prediction of inelastic direct photoproduction, a proper z cut should be taken. We take $0.3 \lesssim z \lesssim 0.9$, which accounts for a clean sample of inelastic direct photoproduction [55,56]. The cross sections for various diquark configurations and production channels under this cut are listed in Table IV.

TABLE IV. Variation for the total cross sections (in unit pb) for the photoproduction of $\Xi_{QQ'}$ at the $\sqrt{S} = 1.30$ TeV LHeC under the cut $0.3 \lesssim z \lesssim 0.9$.

…	$0.3 \lesssim z \lesssim 0.9$			
…	$\langle bb\rangle_{\mathbf{c}}$	$\langle cc\rangle_{\mathbf{c}}$	$\langle bc\rangle_{\bar{\mathbf{3}}}$	$\langle bc\rangle_{\mathbf{6}}$
$\sigma_{\gamma g}$	0.01	10.36	0.98	0.47
$\sigma_{\gamma c}$	…	23.75	0.12	0.06
$\sigma_{\gamma b}$	0.01	…	2.32	1.16
$\sigma^*_{\gamma g}$	0.18	144.82	0.98	1.78
$\sigma^*_{\gamma c}$	…	368.98	0.92	0.46
$\sigma^*_{\gamma b}$	0.23	…	10.65	5.33
Total	0.43	547.91	25.23	

C. Theoretical uncertainties

In this subsection, we make a discussion on the uncertainties caused by the c-quark mass, the b-quark mass, the renormalization (factorization) scale, and the electron scattering angle cut θ_c. All the other parameters are fixed as their center values when discussing the uncertainty from in variation of one parameter.

We present the cross sections at the $\sqrt{S} = 1.30$ TeV LHeC for $m_c = 1.80 \pm 0.10$ GeV and $m_b = 5.10 \pm 0.20$ GeV in Table V. By adding those two errors in quadrature and summing up all the diquark configurations and production channels together, we obtain

$$\sigma^{\text{Total}}_{\langle bb\rangle} = 0.67^{+0.14}_{-0.11}\ \text{pb},$$
$$\sigma^{\text{Total}}_{\langle cc\rangle} = 880.61^{+308.22}_{-219.83}\ \text{pb},$$
$$\sigma^{\text{Total}}_{\langle bc\rangle} = 46.29^{+12.06}_{-9.18}\ \text{pb}.$$

To discuss the scale uncertainty, we set the factorization scale as the renormalization scale, $\mu_f = \mu_r = \mu$. In addition to the scale choice of $\mu = M_T$, we adopt two other scale choices $\mu = 0.75 M_T$ and $\mu = 1.25 M_T$ for discussing the

TABLE V. Variations for the total cross sections (in units pb) for the photoproduction of $\Xi_{QQ'}$ at the $\sqrt{S} = 1.30$ TeV LHeC with $m_c = 1.80 \pm 0.10$ GeV and $m_b = 5.10 \pm 0.20$ GeV. m_b is fixed to 5.10 GeV when discussing the uncertainty from m_c, and m_c is fixed to 1.8 GeV when discussing the uncertainty from m_b.

···	$m_c = 1.7$ GeV				$m_c = 1.9$ GeV				$m_b = 4.9$ GeV				$m_b = 5.3$ GeV			
···	$\langle bb\rangle_{\mathbf{c}}$	$\langle cc\rangle_{\mathbf{c}}$	$\langle bc\rangle_{\bar{\mathbf{3}}}$	$\langle bc\rangle_{\mathbf{6}}$	$\langle bb\rangle_{\mathbf{c}}$	$\langle cc\rangle_{\mathbf{c}}$	$\langle bc\rangle_{\bar{\mathbf{3}}}$	$\langle bc\rangle_{\mathbf{6}}$	$\langle bb\rangle_{\mathbf{c}}$	$\langle cc\rangle_{\mathbf{c}}$	$\langle bc\rangle_{\bar{\mathbf{3}}}$	$\langle bc\rangle_{\mathbf{6}}$	$\langle bb\rangle_{\mathbf{c}}$	$\langle cc\rangle_{\mathbf{c}}$	$\langle bc\rangle_{\bar{\mathbf{3}}}$	$\langle bc\rangle_{\mathbf{6}}$
$\sigma_{\gamma g}$	0.02	30.90	1.84	1.28	0.02	15.38	1.31	0.89	0.03	21.61	1.78	1.21	0.02	21.61	1.35	0.94
$\sigma_{\gamma c}$	···	56.59	0.28	0.14	···	32.84	0.25	0.13	···	42.91	0.32	0.15	···	42.91	0.23	0.11
$\sigma_{\gamma b}$	0.02	···	5.04	2.52	0.02	···	2.98	1.49	0.03	···	3.28	1.64	0.02	···	4.32	2.16
$\sigma^*_{\gamma g}$	0.29	344.37	6.03	5.14	0.29	172.61	4.33	3.67	0.37	241.67	5.87	4.97	0.22	241.67	4.44	3.78
$\sigma^*_{\gamma c}$	···	756.97	1.34	0.67	···	439.95	1.19	0.60	···	574.42	1.48	0.74	···	574.42	1.08	0.54
$\sigma^*_{\gamma b}$	0.34	···	22.61	11.31	0.34	···	13.70	6.85	0.38	···	15.06	7.53	0.30	···	19.49	9.74
Total	0.67	1188.83	58.15		0.67	660.78	37.39		0.81	880.61	44.03		0.56	880.61	48.18	

TABLE VI. Variations for the total cross sections (in unit pb) for the photoproduction of $\Xi_{QQ'}$ at the $\sqrt{S} = 1.30$ TeV LHeC under the renormalization/factorization scale set at $\mu = 0.75 M_T$ and $\mu = 1.25 M_T$.

···	$\mu = 0.75 M_T$				$\mu = 1.25 M_T$			
···	$\langle bb\rangle_{\mathbf{c}}$	$\langle cc\rangle_{\mathbf{c}}$	$\langle bc\rangle_{\bar{\mathbf{3}}}$	$\langle bc\rangle_{\mathbf{6}}$	$\langle bb\rangle_{\mathbf{c}}$	$\langle cc\rangle_{\mathbf{c}}$	$\langle bc\rangle_{\bar{\mathbf{3}}}$	$\langle bc\rangle_{\mathbf{6}}$
$\sigma_{\gamma g}$	0.03	24.57	1.79	1.23	0.02	19.61	1.39	0.96
$\sigma_{\gamma c}$	···	46.21	0.29	0.15	···	39.94	0.25	0.12
$\sigma_{\gamma b}$	0.02	···	2.09	1.04	0.03	···	4.45	2.23
$\sigma^*_{\gamma g}$	0.33	272.55	5.87	4.97	0.26	220.26	4.57	3.89
$\sigma^*_{\gamma c}$	···	617.91	1.38	0.69	···	534.66	1.17	0.59
$\sigma^*_{\gamma b}$	0.30	···	9.50	4.75	0.35	···	20.24	10.12
Total	0.68	961.24	33.75		0.66	814.47	49.98	

TABLE VII. Variations for the total cross sections (in unit pb) for the photoproduction of $\Xi_{QQ'}$ at the $\sqrt{S} = 1.30$ TeV LHeC by setting the electron scattering angle cut $\theta_c = 64$ and 16 mrad.

···	$\theta_c = 16$ mrad				$\theta_c = 64$ mrad			
···	$\langle bb\rangle_{\mathbf{c}}$	$\langle cc\rangle_{\mathbf{c}}$	$\langle bc\rangle_{\bar{\mathbf{3}}}$	$\langle bc\rangle_{\mathbf{6}}$	$\langle bb\rangle_{\mathbf{c}}$	$\langle cc\rangle_{\mathbf{c}}$	$\langle bc\rangle_{\bar{\mathbf{3}}}$	$\langle bc\rangle_{\mathbf{6}}$
$\sigma_{\gamma g}$	0.02	20.08	1.43	0.98	0.03	23.13	1.66	1.14
$\sigma_{\gamma c}$	···	39.98	0.25	0.12	···	45.84	0.29	0.14
$\sigma_{\gamma b}$	0.02	···	3.56	1.78	0.03	···	4.13	2.06
$\sigma^*_{\gamma g}$	0.26	224.83	4.71	4.00	0.31	258.54	5.47	4.64
$\sigma^*_{\gamma c}$	···	535.40	1.17	0.59	···	613.45	1.35	0.68
$\sigma^*_{\gamma b}$	0.31	···	16.18	8.09	0.36	···	18.77	9.39
Total	0.61	820.29	42.86		0.73	940.96	49.72	

scale uncertainty. The scale uncertainty for each diquark configuration and production channel is presented in Table VI. The scale uncertainties for the total cross sections are ~1%, ~9%, and ~27% for Ξ_{bb}, Ξ_{cc}, and Ξ_{bc}, respectively, and we can reduce the scale dependence if we know the β_i-terms of the pQCD series through a next-to-leading order calculation [57,58].

As a final remark, we make a discussion on the uncertainties from the electron scattering angle cut θ_c. For the purpose, we set $\theta_c = 16$ and 64 mrad. The results are shown in Table VII. Within those choices, Table VII shows the uncertainties from θ_c are ~9% for Ξ_{bb}, ~7% for Ξ_{cc}, and ~7% for Ξ_{bc}. The small uncertainty from θ_c shows the WWA is appropriate choice for our calculation.

IV. SUMMARY

In the paper, the photoproduction of doubly heavy baryon at the LHeC via the channels $\gamma + g \to \Xi_{QQ'} + \bar{Q} + \bar{Q}'$ and $\gamma + Q \to \Xi_{QQ'} + \bar{Q}'$ has been studied within the framework of NRQCD.

We have found the extrinsic heavy quark mechanism via $\gamma + Q \to \Xi_{QQ'} + \bar{Q}'$ provides a significant production rate comparing to the channel $\gamma + g \to \Xi_{QQ'} + \bar{Q} + \bar{Q}'$, regardless of the suppressions from the heavy quark PDFs. There are four spin-and-color diquark configurations for the production of doubly heavy baryons, i.e., $[^1S_0]_{\bar{\mathbf{3}}/\mathbf{6}}$ and $[^3S_1]_{\bar{\mathbf{3}}/\mathbf{6}}$. It was found that the $[^3S_1]_{\bar{\mathbf{3}}}$-diquark state provides dominate contribution to the $\Xi_{QQ'}$ production. While other diquark states can also provide sizable contributions to the $\Xi_{QQ'}$ production, thus a careful discussion of all diquark configurations are helpful for a sound prediction of the doubly heavy baryon production.

The cross sections and its uncertainties caused by different choices of the heavy-quark mass, the renormalization/factorization scale and θ_c are presented. By taking $m_c = 1.80 \pm 0.10$ GeV and $m_b = 5.1 \pm 0.20$ GeV, we shall have $(6.70^{+1.40}_{-1.10}) \times 10^3$ Ξ_{bb}, $(8.81^{+3.08}_{-2.20}) \times 10^6$ Ξ_{cc}, and $(4.63^{+1.21}_{-0.92}) \times 10^5$ Ξ_{bc} events to be generated in one operation year at the LHeC under the condition of $\sqrt{S} = 1.30$ TeV and $\mathcal{L} \simeq 10^{33}$ cm^{-2} s^{-1}, where all diquark

configurations and production channels have been summing up. With such amounts of production rate, the LHeC and its updated version, the FCC-ep, shall provide a helpful platform for studying the properties of doubly heavy baryon, especially for Ξ_{cc} and Ξ_{bc}.

At last, we make a discussion about the light quark component in the doubly heavy baryon $\Xi_{QQ'q}$, where q denotes light quark u, d, or s, respectively. The ratio for a diquark $\langle QQ'\rangle[n]$ evolving to a certain doubly heavy baryon $\Xi_{QQ'u}$, $\Xi_{QQ'd}$, or $\Xi_{QQ's}$ is about 1:1:0.3 [59]. Thus, 43% of $\langle cc\rangle[n]$ are to be fragmented into Ξ_{cc}^{++}, 43% for Ξ_{cc}^{+}, and 14% for Ω_{cc}^{+}. The same estimation occurs for the production of Ξ_{bb}^{0}, Ξ_{bb}^{-}, and Ω_{bb}^{-} or the production of Ξ_{bc}^{+}, Ξ_{bc}^{0}, and Ω_{bc}^{0}.

ACKNOWLEDGMENTS

This work was supported in part by the National Natural Science Foundation of China (No. 11375171, No. 11405173, No. 11535002 and No. 11625520). The authors would like to thank Xu-Chang Zheng for helpful discussion.

[1] G. T. Bodwin, E. Braaten, and G. P. Lepage, Rigorous QCD analysis of inclusive annihilation and production of heavy quarkonium, Phys. Rev. D **51**, 1125 (1995); Erratum, Phys. Rev. D **55**, 5853(E) (1997).
[2] N. Brambilla *et al.* (Quarkonium Working Group Collaboration), Heavy quarkonium physics, arXiv:hep-ph/0412158.
[3] N. Brambilla *et al.*, Heavy quarkonium: Progress, puzzles, and opportunities, Eur. Phys. J. C **71**, 1534 (2011).
[4] J. L. Abelleira Fernandez *et al.* (LHeC Study Group Collaboration), A Large Hadron Electron Collider at CERN: Report on the physics and design concepts for machine and detector, J. Phys. G **39**, 075001 (2012).
[5] H. Y. Bi, R. Y. Zhang, H. Y. Han, Y. Jiang, and X. G. Wu, Photoproduction of the $B_c^{(*)}$ meson at the LHeC, Phys. Rev. D **95**, 034019 (2017).
[6] M. Mattson *et al.* (SELEX Collaboration), First Observation of the Doubly Charmed Baryon Ξ_{cc}^{+}, Phys. Rev. Lett. **89**, 112001 (2002).
[7] M. A. Moinester (SELEX Collaboration), First observation of doubly charmed baryons, Czech. J. Phys. **53**, B201 (2003).
[8] A. Ocherashvili *et al.* (SELEX Collaboration), Confirmation of the doubly charmed baryon $\Xi_{cc}^{+}(3520)$ via its decay to $pD^{+}K^{-}$, Phys. Lett. B **628**, 18 (2005).
[9] M. A. Doncheski, J. Steegborn, and M. L. Stong, Fragmentation production of doubly heavy baryons, Phys. Rev. D **53**, 1247 (1996).
[10] M. A. Moinester, How to search for doubly charmed baryons and tetraquarks, Z. Phys. A **355**, 349 (1996).
[11] S. P. Baranov, Production of doubly flavored baryons in pp, ep and $\gamma\gamma$ collisions, Phys. Rev. D **54**, 3228 (1996).
[12] A. V. Berezhnoy, V. V. Kiselev, and A. K. Likhoded, Hadronic production of baryons containing two heavy quarks, Phys. At. Nucl. **59**, 870 (1996).
[13] A. V. Berezhnoy, V. V. Kiselev, A. K. Likhoded, and A. I. Onishchenko, Doubly charmed baryon production in hadronic experiments, Phys. Rev. D **57**, 4385 (1998).
[14] V. V. Kiselev and A. K. Likhoded, Baryons with two heavy quarks, Phys. Usp. **45**, 455 (2002).
[15] C. H. Chang, C. F. Qiao, J. X. Wang, and X. G. Wu, Estimate of the hadronic production of the doubly charmed baryon Ξ_{cc} in the general-mass variable-flavor-number scheme, Phys. Rev. D **73**, 094022 (2006).
[16] C. H. Chang, J. P. Ma, C. F. Qiao, and X. G. Wu, Hadronic production of the doubly charmed baryon Ξ_{cc} with intrinsic charm, J. Phys. G **34**, 845 (2007).
[17] A. F. Falk, M. E. Luke, M. J. Savage, and M. B. Wise, Heavy quark fragmentation to baryons containing two heavy quarks, Phys. Rev. D **49**, 555 (1994).
[18] J. P. Ma and Z. G. Si, Factorization approach for inclusive production of doubly heavy baryon, Phys. Lett. B **568**, 135 (2003).
[19] S. Koshkarev and V. Anikeev, Production of the doubly charmed baryons at the SELEX experiment—The double intrinsic charm approach, Phys. Lett. B **765**, 171 (2017).
[20] C. H. Chang, J. X. Wang, and X. G. Wu, GENXICC: A generator for hadronic production of the double heavy baryons Ξ_{cc}, Ξ_{bc} and Ξ_{bb}, Comput. Phys. Commun. **177**, 467 (2007).
[21] C. H. Chang, J. X. Wang, and X. G. Wu, GENXICC2.0: An upgraded version of the generator for hadronic production of double heavy baryons Ξ_{cc}, Ξ_{bc} and Ξ_{bb}, Comput. Phys. Commun. **181**, 1144 (2010).
[22] X. Y. Wang and X. G. Wu, GENXICC2.1: An improved version of GENXICC for hadronic production of doubly heavy baryons, Comput. Phys. Commun. **184**, 1070 (2013).
[23] J. W. Zhang, X. G. Wu, T. Zhong, Y. Yu, and Z. Y. Fang, Hadronic production of the doubly heavy baryon Ξ_{bc} at the LHC, Phys. Rev. D **83**, 034026 (2011).
[24] G. Chen, X. G. Wu, J. W. Zhang, H. Y. Han, and H. B. Fu, Hadronic production of Ξ_{cc} at a fixed-target experiment at the LHC, Phys. Rev. D **89**, 074020 (2014).
[25] R. Aaij *et al.* (LHCb Collaboration), Search for the doubly charmed baryon Ξ_{cc}^{+}, J. High Energy Phys. 12 (2013) 090.
[26] J. P. Ma and C. H. Chang, Preface: Z-factory, Sci. China-Phys. Mech. Astron. **53**, 1947 (2010).
[27] G. Aarons *et al.* (ILC Collaboration), International Linear Collider reference design report volume 2: Physics at the ILC, arXiv:0709.1893.
[28] J. Jiang, X. G. Wu, Q. L. Liao, X. C. Zheng, and Z. Y. Fang, Doubly heavy baryon production at a high luminosity $e^{+}e^{-}$ collider, Phys. Rev. D **86**, 054021 (2012).

[29] J. Jiang, X. G. Wu, S. M. Wang, J. W. Zhang, and Z. Y. Fang, Further study on the doubly heavy baryon production around the Z^0 peak at a high luminosity e^+e^- collider, Phys. Rev. D **87**, 054027 (2013).
[30] X. C. Zheng, C. H. Chang, and Z. Pan, Production of doubly heavy-flavored hadrons at e^+e^- colliders, Phys. Rev. D **93**, 034019 (2016).
[31] G. Chen, X. G. Wu, Z. Sun, Y. Ma, and H. B. Fu, Photoproduction of doubly heavy baryon at the ILC, J. High Energy Phys. 12 (2014) 018.
[32] S. J. Brodsky, C. Peterson, and N. Sakai, Intrinsic heavy-quark states, Phys. Rev. D **23**, 2745 (1981).
[33] S. J. Brodsky, P. Hoyer, C. Peterson, and N. Sakai, The intrinsic charm of the proton, Phys. Lett. **93B**, 451 (1980).
[34] C. F. von Weizsacker, Radiation emitted in collisions of very fast electrons, Z. Phys. **88**, 612 (1934).
[35] E. J. Williams, Nature of the high-energy particles of penetrating radiation and status of ionization and radiation formulae, Phys. Rev. **45**, 729 (1934).
[36] S. Frixione, M. L. Mangano, P. Nason, and G. Ridolfi, Improving the Weizsacker-Williams approximation in electron—proton collisions, Phys. Lett. B **319**, 339 (1993).
[37] F. I. Olness, R. J. Scalise, and W. K. Tung, Heavy quark hadroproduction in perturbative QCD, Phys. Rev. D **59**, 014506 (1998).
[38] M. A. G. Aivazis, F. I. Olness, and W. K. Tung, Leptoproduction of heavy quarks. 1. General formalism and kinematics of charged current and neutral current production processes, Phys. Rev. D **50**, 3085 (1994).
[39] M. A. G. Aivazis, J. C. Collins, F. I. Olness, and W. K. Tung, Leptoproduction of heavy quarks. 2. A Unified QCD formulation of charged and neutral current processes from fixed target to collider energies, Phys. Rev. D **50**, 3102 (1994).
[40] J. Amundson, C. Schmidt, W. K. Tung, and X. Wang, Charm production in deep inelastic scattering from threshold to high Q^2, J. High Energy Phys. 10 (2000) 031.
[41] B. A. Kniehl, G. Kramer, I. Schienbein, and H. Spiesberger, Collinear subtractions in hadroproduction of heavy quarks, Eur. Phys. J. C **41**, 199 (2005).
[42] M. Klasen, T. Kleinwort, and G. Kramer, Inclusive jet production in γp and $\gamma\gamma$ processes: Direct and resolved photon cross sections in next-to-leading order QCD, Eur. Phys. J. direct C **1**, 1 (2000).
[43] M. Klasen, Theory of hard photoproduction, Rev. Mod. Phys. **74**, 1221 (2002).
[44] T. Hahn, Generating Feynman diagrams and amplitudes with FeynArts 3, Comput. Phys. Commun. **140**, 418 (2001).
[45] R. Mertig, M. Bohm, and A. Denner, Feyn Calc: Computer-algebraic calculation of Feynman amplitudes, Comput. Phys. Commun. **64**, 345 (1991).
[46] V. Shtabovenko, R. Mertig, and F. Orellana, New developments in FeynCalc 9.0, Comput. Phys. Commun. **207**, 432 (2016).
[47] F. Feng and R. Mertig, FormLink/FeynCalcFormLink: Embedding FORM in Mathematica and FeynCalc, arXiv: 1212.3522.
[48] G. P. Lepage, A new algorithm for adaptive multidimensional integration, J. Comput. Phys. **27**, 192 (1978).
[49] T. Hahn and M. Perez-Victoria, Automatized one loop calculations in four and D dimensions, Comput. Phys. Commun. **118**, 153 (1999).
[50] E. Bagan, H. G. Dosch, P. Gosdzinsky, S. Narison, and J. M. Richard, Hadrons with charm and beauty, Z. Phys. C **64**, 57 (1994).
[51] C. F. Qiao and J. X. Wang, $J/\psi + c + \bar{c}$ photoproduction in e^+e^- scattering, Phys. Rev. D **69**, 014015 (2004).
[52] R. Li and K. T. Chao, Photoproduction of J/ψ in association with a $c\bar{c}$ pair, Phys. Rev. D **79**, 114020 (2009).
[53] H. L. Lai, M. Guzzi, J. Huston, Z. Li, P. M. Nadolsky, J. Pumplin, and C.-P. Yuan, New parton distributions for collider physics, Phys. Rev. D **82**, 074024 (2010).
[54] Y. C. Acar, A. N. Akay, S. Beser, H. Karadeniz, U. Kaya, B. B. Oner, and S. Sultansoy, FCC based lepton-hadron and photon-hadron colliders: Luminosity and physics, arXiv: 1608.02190.
[55] M. Kramer, QCD corrections to inelastic J/ψ photoproduction, Nucl. Phys. **B459**, 3 (1996).
[56] C. Adloff *et al.* (H1 Collaboration), Inelastic photoproduction of J/ψ mesons at HERA, Eur. Phys. J. C **25**, 25 (2002).
[57] X. G. Wu, S. J. Brodsky, and M. Mojaza, The renormalization scale-setting problem in QCD, Prog. Part. Nucl. Phys. **72**, 44 (2013).
[58] X. G. Wu, Y. Ma, S. Q. Wang, H. B. Fu, H. H. Ma, S. J. Brodsky, and M. Mojaza, Renormalization group invariance and optimal QCD renormalization scale-setting: A key issues review, Rep. Prog. Phys. **78**, 126201 (2015).
[59] T. Sjostrand, S. Mrenna, and P. Z. Skands, PYTHIA 6.4 physics and manual, J. High Energy Phys. 05 (2006) 026.